

Thioredoxin-interacting protein regulates insulin transcription through microRNA-204

Guanlan Xu, Junqin Chen, Gu Jing & Anath Shalev

Beta-cell dysfunction and impaired insulin production are hallmarks of diabetes¹, but despite the growing diabetes epidemic, the molecular mechanisms underlying this disease have remained unclear. We identified thioredoxin-interacting protein (TXNIP), a cellular redox regulator, as a crucial factor in beta-cell biology and show that beta-cell TXNIP is upregulated in diabetes, whereas TXNIP deficiency protects against diabetes by preventing beta-cell apoptosis^{2,3}. Here we show that TXNIP and diabetes induce beta-cell expression of a specific microRNA, miR-204, which in turn blocks insulin production by directly targeting and downregulating *MAFA*, a known insulin transcription factor. In particular, we first discovered the regulation of miR-204 by TXNIP by microarray analysis, followed by validation studies in INS-1 beta cells, islets of Txnip-deficient mice, diabetic mouse models and primary human islets. We then further found that TXNIP induces miR-204 by inhibiting the activity of signal transducer and activator of transcription 3 (STAT3), a transcription factor that is involved in miR-204 regulation^{4,5}. We also identified *MAFA* as a target that is downregulated by miR-204. Taken together, our results demonstrate that TXNIP controls microRNA expression and insulin production and that miR-204 is involved in beta-cell function. The newly identified TXNIP–miR-204–MAFA–insulin pathway may contribute to diabetes progression and provides new insight into TXNIP function and microRNA biology in health and disease.

Production and release of adequate amounts of insulin by pancreatic beta cells is a prerequisite for maintaining normal glucose homeostasis. Indeed, beta-cell dysfunction and impaired insulin production are key factors in the pathogenesis of diabetes¹, but despite the growing worldwide diabetes epidemic, the molecular mechanisms involved in this disease process have only begun to be discovered. Recently we identified TXNIP, a cellular redox regulator⁶, as a crucial factor in beta-cell biology. In particular, we previously showed that beta-cell TXNIP was upregulated in diabetes, whereas TXNIP deficiency protected against type 1 and type 2 diabetes by preventing beta-cell apoptosis and increasing whole-pancreas beta-cell mass^{2,3,7–11}. Furthermore, we revealed the pathways by which TXNIP induces apoptosis^{2,10} and discovered that TXNIP shuttles within the beta

cell and translocates from the nucleus into the mitochondria, where it initiates the mitochondrial apoptotic cascade¹⁰. The discovery that under normal conditions TXNIP is localized primarily in the nucleus combined with our previous gene expression profiling studies demonstrating that ~95% of all altered genes are downregulated by TXNIP⁹ raised the possibility that TXNIP might be involved in the control (particularly the inhibition) of beta-cell gene expression, which prompted us to study the potential effects of TXNIP on microRNA expression.

MicroRNAs (small 20- to 24-nt noncoding RNAs) recognize and bind target mRNAs through imperfect base pairing, which leads to mRNA degradation or translational inhibition of the target mRNA and downregulation of target gene expression^{12–14}. MicroRNAs are rapidly emerging as important regulators of gene expression in health and disease and were also recently discovered to have various roles in diabetes and beta-cell biology^{15–21}.

Comparison of our TXNIP-overexpressing INS-1 beta-cell line (INS-TXNIP) and a control INS-1 beta-cell line expressing LacZ (INS-LacZ) using miRCURY LNA microRNA Arrays (Exiqon) and an absolute difference threshold of 0.7 in LogMedianRatio (1.6-fold change) revealed five microRNAs (miR-139-5p, miR-193, miR-204, miR-200c and miR-141) that were upregulated in response to TXNIP overexpression (**Supplementary Table 1**). After confirming these findings by quantitative real-time PCR, we investigated the role of these microRNAs by systematically knocking them down using specific inhibitor oligonucleotides and assessing the effects on insulin production, a key aspect of beta-cell function. However, only knock-down of miR-204 had a significant ($P < 0.05$) effect and led to an increase in insulin expression. Moreover, only overexpression of miR-204, but not any of the other microRNAs, resulted in a marked decrease in insulin mRNA expression (**Supplementary Fig. 1a**).

Notably, miR-204 (which is fully conserved between human, rat and mouse) (**Supplementary Fig. 1b**) has not been implicated in beta-cell biology but is highly expressed in insulinomas²². Consistent with this observation, miR-204 was readily detectable in INS-1 cells, but in agreement with the results from the other microRNAs, its expression was even higher in primary human islets, whereas its expression in mouse islets was lower than in INS-1 cells (**Supplementary Fig. 1c**). Of note, human pancreatic islets are also one of the major sites of miR-204 expression according to the microRNA.org website,

Comprehensive Diabetes Center, Department of Medicine, Division of Endocrinology, Diabetes and Metabolism, University of Alabama at Birmingham, Birmingham, Alabama, USA. Correspondence should be addressed to A.S. (shalev@uab.edu).

Received 2 January; accepted 1 July; published online 25 August 2013; doi:10.1038/nm.3287

Figure 1 The effects of TXNIP and diabetes on beta-cell miR-204 expression. (a–c) Expression of miR-204, as assessed by qRT-PCR in INS-1 cells overexpressing TXNIP (INS-TXNIP) and control cells (INS-LacZ) (a), primary islets of *Txnip*-deficient HcB-19 and C3H control mice (b) and primary islets of beta cell-specific *Txnip* knockout (bTKO) and *lox/lox* control mice (c). (d) The effects of TXNIP on STAT3 activation determined by immunoblotting for pSTAT3 and total STAT3 in INS-TXNIP and control INS-LacZ cells. (e) The expression of miR-204, detected by qRT-PCR, in INS-1 cells that were incubated with the STAT3 inhibitor STATTC (2 μ M for 48 h) or vehicle (DMSO). (f) The expression of miR-204, analyzed by qRT-PCR, in primary islets of 10-week-old male diabetic *ob/ob* or lean control mice. All data are shown as the mean \pm s.e.m. of 3–5 independent experiments. * $P < 0.05$, ** $P < 0.01$ (Student's *t* test).

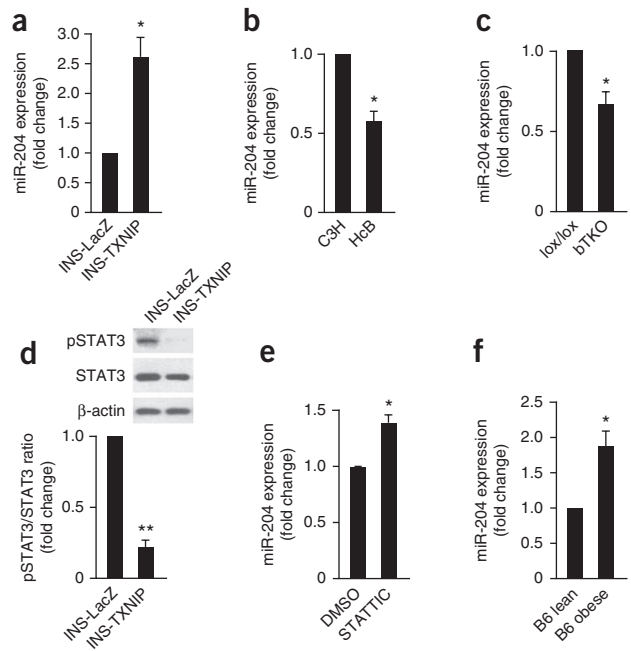
but the function and target genes of miR-204 are unknown. Taken together, these findings suggest that miR-204 might have an important role in beta-cell biology, and we therefore decided to focus on this microRNA.

Using quantitative real-time RT-PCR (qRT-PCR), we found that miR-204 expression was over twofold higher in INS-TXNIP cells as compared to its expression in control INS-LacZ cells (Fig. 1a), confirming our microarray findings. In contrast, primary islets from *Txnip*-deficient HcB-19 mice (which harbor a natural nonsense mutation in the *Txnip* gene) showed significantly lower miR-204 expression as compared to C3H control mice (Fig. 1b). Similarly, miR-204 expression was significantly lower in islets from our beta-cell-specific *Txnip* knockout (bTKO) mice as compared to *lox/lox* control mice (Fig. 1c), further indicating that TXNIP regulates miR-204 expression in beta cells *in vivo*.

Encoded within intron 6 of the *TRPM3* gene (transient receptor potential melastatin 3, a cation-selective channel), miR-204 is transcribed in the same direction as *TRPM3* (ref. 23). Because miR-204 and *TRPM3* therefore share the same promoter, we hypothesized that if TXNIP regulates miR-204 expression at the transcriptional level, *TRPM3* would be co-regulated in parallel. Indeed, we found that *Trpm3* expression was more than threefold higher in TXNIP-overexpressing INS-TXNIP cells as compared to its expression in control INS-LacZ cells (Supplementary Fig. 1d), whereas primary islets from *Txnip*-deficient HcB-19 mice showed a significant ($P < 0.05$) reduction in *Trpm3* expression (Supplementary Fig. 1e). These findings are similar to results obtained for miR-204 and suggest that TXNIP upregulates miR-204 by inducing its transcription.

As TXNIP is not known to act as a transcription factor, we hypothesized that it acts through the regulation of another factor. STAT3 was recently implicated in the downregulation of miR-204 expression by some studies^{4,5}, and given the observed upregulation of miR-204 in response to TXNIP, we investigated whether TXNIP might inhibit STAT3. Indeed, although TXNIP had no effect on *Stat3* mRNA expression (Supplementary Fig. 1g) or total protein amounts, Stat3 phosphorylation and activation (which is crucial for STAT3-mediated transcription) were substantially reduced in response to TXNIP (Fig. 1d). Using STATTC, a small molecule that selectively inhibits the activation of the STAT3 transcription factor by blocking its phosphorylation and dimerization, we investigated whether it could mimic the effects of TXNIP. We found that similarly to TXNIP, STATTC significantly induced miR-204 expression (Fig. 1e), as well as that of its host gene, *Trpm3* (Supplementary Fig. 1f), suggesting that TXNIP confers its effects on miR-204 at least in part through inhibition of STAT3.

Given the involvement of TXNIP in diabetes^{3,8,24}, we investigated whether miR-204 expression in beta cells might also be altered in

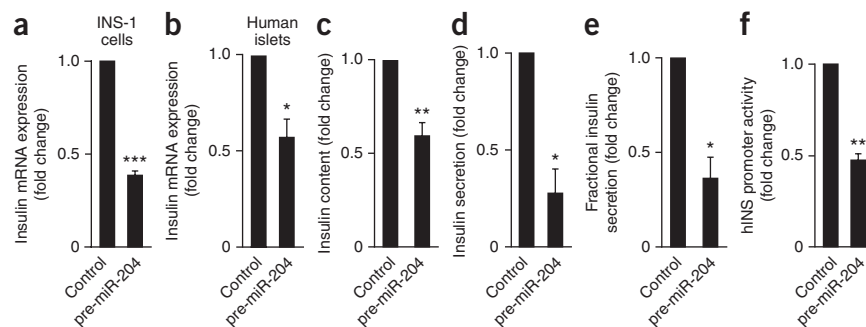


diabetes. We used the well-established *ob/ob* mouse model, which is obese and diabetic as a result of leptin deficiency, in the C57/B6 background (B6 *ob/ob*) as a model of type 2 diabetes (Supplementary Fig. 2a,b). Islets of obese and diabetic mice showed markedly elevated expression of *Txnip* (Supplementary Fig. 2c). Most notably, miR-204 expression was significantly higher in diabetic B6 *ob/ob* mice compared to lean control mice (Fig. 1f), suggesting that this microRNA might have a role in the beta-cell dysfunction of diabetes. Of note, we also found that miR-204 expression was significantly ($P < 0.05$) elevated in two additional models of diabetes: BTBR *ob/ob* and A-ZIP/F-1 mice (Supplementary Fig. 3a–f). Unlike B6 *ob/ob* mice, which typically have rather mild diabetes, BTBR *ob/ob* mice are not able to compensate for their leptin deficiency-induced obesity and insulin resistance and develop severe type 2 diabetes that is consistent with a more pronounced islet phenotype that includes disrupted islet architecture and reduced whole-pancreas insulin content²⁵. In contrast, A-ZIP/F-1 mice are not obese and lack white adipose tissue (because of adipose-specific transgenic expression of a dominant-negative protein (A-ZIP/F) that blocks C/EBP and Jun-mediated transcription) but are severely diabetic²⁶. Despite these differences, both models showed higher *Txnip* expression, consistent with our previous findings^{3,8}, and higher miR-204 levels compared to nondiabetic controls.

Given the proapoptotic effects of TXNIP, we also tested the possibility that miR-204 might induce beta-cell apoptosis. However, compared to scrambled control microRNA, overexpression of miR-204 did not result in a significant increase in the ratio of *Bax* to *Bcl2* expression levels ($P = 0.313$), an increase in the amount of cleaved caspase-3 or an increase in the number of TUNEL positive beta cells (data not shown), indicating that unlike TXNIP, miR-204 does not induce beta-cell apoptosis. We therefore tested how miR-204 might affect other aspects of beta-cell function, such as insulin production.

Overexpression of miR-204 in INS-1 cells led to a >200% reduction in insulin mRNA expression (Fig. 2a). Unlike humans, rodents have two insulin genes (*Ins1* and *Ins2*), and although the data shown were obtained with primers detecting expression from both rat insulin genes, unless otherwise noted, primers specific for either *Ins1* or *Ins2* showed the same effect. In human islets, miR-204 overexpression led

Figure 2 The effects of miR-204 on insulin production. (a,b) Insulin mRNA expression, determined by qRT-PCR, in INS-1 cells (a) and human islets (b) that were transfected with miR-204 precursor (pre-miR-204) or scrambled control microRNA and analyzed after 72 h. (c,d) Cellular insulin protein content (c) and insulin secretion (d) in INS-1 cells overexpressing miR-204 or scrambled control microRNA assessed by ELISA and normalized for cellular DNA content. (e) Fractional insulin secretion calculated by normalizing insulin secretion to insulin content. (f) Insulin promoter activity, assessed by firefly luciferase and corrected for transfection efficiency with the pRL-TK *Renilla* luciferase-expressing control plasmid, in INS-1 cells that were cotransfected with the human insulin promoter reporter construct *Ins-luc* (hINS) and pre-miR-204 or scrambled control and analyzed 72 h later. All data are shown as the mean \pm s.e.m. of three independent experiments. * $P < 0.05$, ** $P < 0.01$, *** $P < 0.001$ (Student's *t* test).



to a similar decrease in insulin mRNA expression as in INS-1 cells (Fig. 2b), demonstrating that this effect is also relevant to human islet biology. In addition, the decrease in insulin mRNA expression translated into significantly reduced insulin content in miR-204-overexpressing cells at the protein level (Fig. 2c), as well as decreased insulin secretion (Fig. 2d) and fractional insulin secretion (Fig. 2e; control insulin content was 7.5 and secretion was 1.7 ng ml⁻¹ per μ g DNA). The latter finding suggests that miR-204 might have additional direct effects on insulin secretion. Moreover, the higher miR-204 levels observed in the diabetic B6 ob/ob mice were also associated with significantly ($P < 0.05$) lower insulin gene expression (Supplementary Fig. 2d,e). Similarly, elevated miR-204 levels were also associated with reduced insulin gene expression in the two additional diabetes models tested, BTBR ob/ob and A-ZIP/F-1 mice (Supplementary Fig. 3a–f). In contrast, transfection of miR-204 inhibitor oligonucleotides resulted in not only effective inhibition of miR-204 (Supplementary Fig. 3g) but also a significant ($P < 0.05$) increase in insulin mRNA expression (Supplementary Fig. 3h), suggesting that miR-204 regulates insulin gene expression. However, we observed that miR-204 inhibited insulin promoter activity (Fig. 2f) rather than having the classical post-transcriptional effects of microRNAs on mRNA stability or translation. This suggests that the effect was indirect and was probably mediated by miR-204-induced downregulation of factor(s) that are involved in insulin transcription.

To identify these factors, we next set out to find the putative gene targets of miR-204, especially those that might have a role in insulin transcription. We therefore tested whether miR-204 could inhibit the expression of any of the key insulin transcription factors, MAFA, MAFB, NEUROD or PDX1 (refs. 27–29), which also came up as potential targets using miRWalk algorithms. *Mafa* mRNA and protein levels were markedly reduced in response to miR-204 overexpression (Fig. 3a,b), as well as *in vivo* in the context of diabetes-induced miR-204 (Supplementary Fig. 2f), whereas miR-204 inhibition led to a more than twofold increase in *Mafa* expression (Supplementary Fig. 3i). In contrast, the other transcription factors were not significantly altered by overexpression or inhibition of miR-204 (Supplementary Fig. 4a–f).

Although MAFA has been shown to be capable of activating *PDX1* promoter-driven reporter gene expression³⁰, MAFA and *PDX1* are not always coexpressed. Consistent with our findings, *Mafa* expression was previously found to be lower in islets from diabetic, obese, leptin-receptor mutant (db/db) mice compared to nondiabetic controls and in response to c-Jun, whereas *Pdx1* expression remained unchanged in these conditions³¹. In addition, glucose has been shown to induce the expression of *Mafa* but not *Pdx1* in beta cells³². Here,

we found that the miR-204-induced reduction in *Mafa* expression also resulted in substantially reduced *Mafa* binding to the insulin promoter, as assessed by chromatin immunoprecipitation (ChIP) studies (Fig. 3c).

Together these findings raise the possibility that MAFA acts as the miR-204 target, mediating the effects of this microRNA on insulin gene expression. Comparison of the miR-204 seed sequence and the rat *Mafa* 3' untranslated region (UTR) revealed a perfect 7-nt match (Fig. 3d), suggesting that *Mafa* might be a target of miR-204. To address this possibility, we generated reporter constructs with either a wild-type or mutated *Mafa* 3' UTR (Fig. 3d) cloned downstream of the luciferase gene and assessed miR-204-directed repression of the reporter gene. We found that miR-204 significantly decreased luciferase activity through the wild-type *Mafa* 3' UTR, whereas there was no reduction with the mutant 3' UTR construct (Fig. 3e), confirming that *Mafa* is indeed a direct target of miR-204. Of note, MAFA is highly conserved across species at both the protein and mRNA levels, and TargetScan predicted that the rat 3' UTR contains a unique miR-204 binding site, which is consistent with our findings in rat INS-1 beta cells. Furthermore, alignment of the rat, human and mouse 3' UTR sequences revealed that six of the seven nucleotides contained in the miR-204 seed match were also conserved in human and mouse MAFA (Supplementary Table 1), and such matching has been reported to be sufficient for the downregulation of target messages³³. Nevertheless, we also performed reporter assays using plasmids encoding the wild-type human MAFA 3' UTR as well as a human MAFA 3' UTR with a mutated miR-204 binding seed sequence (Supplementary Fig. 4g). The presence of miR-204 led to a small but highly significant ($P < 0.05$) and consistent decrease in luciferase activity through the wild-type human MAFA 3' UTR, and this effect was completely blunted by mutation of the seed sequence (Supplementary Fig. 4h). Moreover, miR-204 also significantly ($P < 0.05$) reduced MAFA expression in human islets (Supplementary Fig. 4i) and led to an almost 50% reduction in human insulin expression (Fig. 2b). This is in line with our findings in rat INS-1 beta cells, demonstrates the translatability of the results and suggests that the miR-204–MAFA–insulin pathway is also active in human islets.

It should be noted that currently, no validated human pancreatic beta cell line is available, making it necessary to use non-beta cell lines or primary human islets with a lower transfection efficiency, which may explain the slightly smaller effect size found in some of these experiments compared to those found using rodent models. Although even small changes in the expression of a transcription factor such as MAFA can lead to much larger effects on target gene expression (for example, insulin (as observed in our human islets)), we cannot exclude

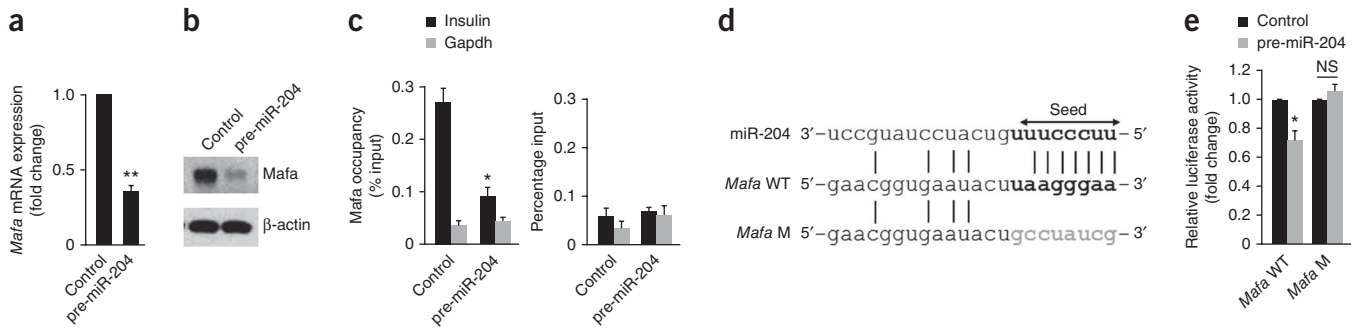


Figure 3 *MAFA* as a target of miR-204. **(a,b)** The effects of miR-204 on *Mafa* mRNA **(a)** and protein **(b)** expression as assessed by qRT-PCR and immunoblotting. **(c)** Changes in the *Mafa* occupancy of the insulin promoter in response to miR-204 as measured by ChIP. IgG control results are shown on the right. Gapdh, glyceraldehyde 3-phosphate dehydrogenase. **(d)** Alignment of the miR-204 seed sequence (arrow) and the wild-type (WT) rat *Mafa* 3' UTR target sequence (bold) and the mutated (M) target sequence (gray). **(e)** miR-204-directed repression of the luciferase reporter gene bearing the WT or mutant *Mafa* 3' UTR segments as assessed 24 h after cotransfecting INS-1 cells with the wild-type or mutant reporter plasmids. All data are shown as the mean \pm s.e.m. of three independent experiments, and one representative immunoblot is shown. * $P < 0.05$, ** $P < 0.01$ (Student's *t* test). NS, not significant.

the possibility that additional factors targeted by miR-204 might be involved in the more complex setting of the human islet.

To investigate whether TXNIP, as an upstream regulator of miR-204, could mimic the effects of miR-204 on *MAFA*, we analyzed our TXNIP-overexpressing INS-1 cell line and found a >200% reduction in *Mafa* mRNA expression and *Mafa* protein amounts (Fig. 4a,b), similarly to what we observed in response to direct miR-204 overexpression. In contrast, TXNIP had no effect on *Pdx1*, *Mafb* or *Neurod* expression (Supplementary Fig. 5a–c). ChIP analysis revealed that *Mafa* occupancy of the insulin promoter in the TXNIP-overexpressing cells was reduced to almost half of that in the INS-LacZ control cells (Fig. 4c). Moreover, TXNIP also reduced *MAFA* expression in human islets (Fig. 4d), confirming the physiological relevance of these findings.

To further test whether TXNIP can block insulin production similarly to miR-204, we conducted parallel experiments using our

TXNIP-overexpressing INS-1 cells, as well as human islets and *Txnip*-deficient HcB-19 mouse islets. TXNIP led to a significant decrease in insulin mRNA expression in the INS-1 cells (Fig. 4e) and human islets (Fig. 4f). This transient TXNIP overexpression in the human islets did not lead to any beta-cell apoptosis, as determined by an unchanged ratio of *Bax* to *Bcl2* expression levels in the same samples, making any confounding effects in this regard extremely unlikely. At the protein level, TXNIP also caused a substantial reduction in insulin content (Fig. 4g) and an associated decrease in insulin secretion (Fig. 4h). This effect seemed to have been caused primarily by the reduced insulin content, as fractional insulin secretion was not significantly affected by TXNIP (Supplementary Fig. 5d). In contrast, islets of *Txnip*-deficient mice showed a highly significant, twofold higher insulin content as compared to C3H control mice (Fig. 4i), strongly supporting the notion that TXNIP inhibits beta-cell insulin

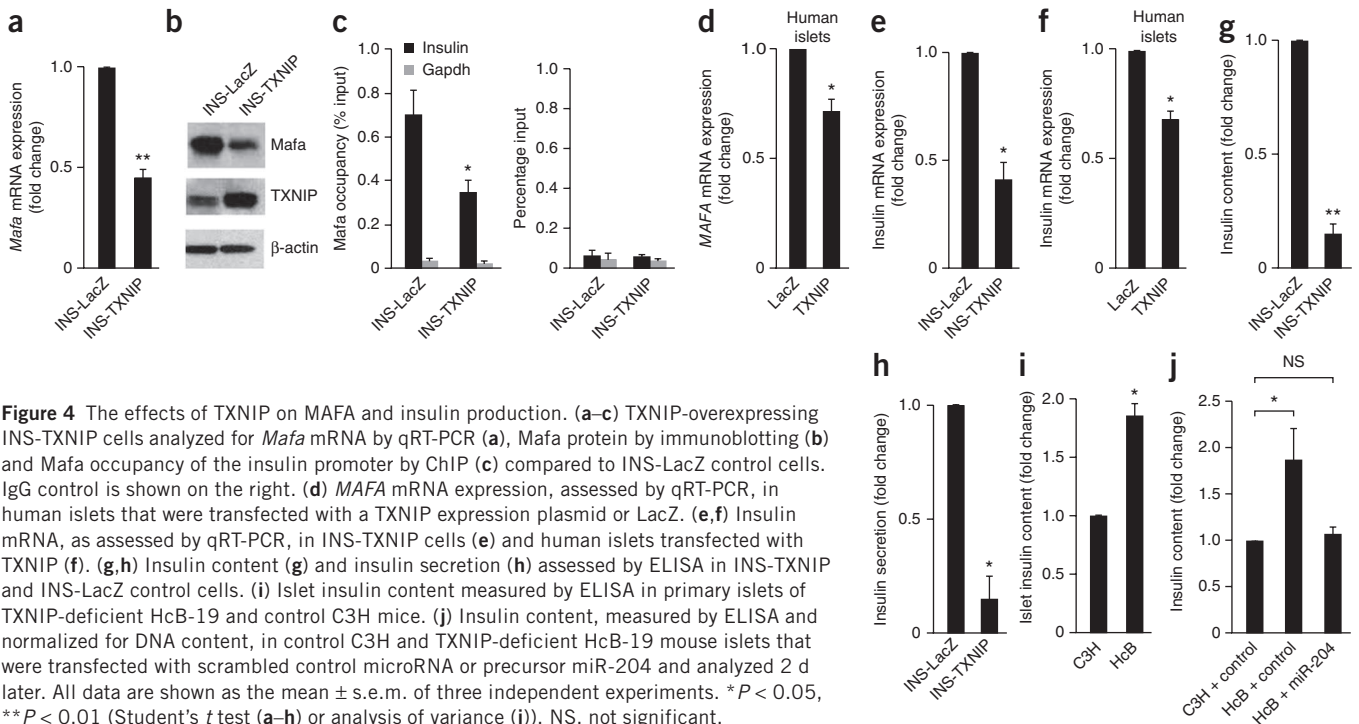


Figure 4 The effects of TXNIP on *MAFA* and insulin production. **(a–c)** TXNIP-overexpressing INS-TXNIP cells analyzed for *Mafa* mRNA by qRT-PCR **(a)**, *Mafa* protein by immunoblotting **(b)** and *Mafa* occupancy of the insulin promoter by ChIP **(c)** compared to INS-LacZ control cells. IgG control is shown on the right. **(d)** *MAFA* mRNA expression, assessed by qRT-PCR, in human islets that were transfected with a TXNIP expression plasmid or LacZ. **(e,f)** Insulin mRNA, as assessed by qRT-PCR, in INS-TXNIP cells **(e)** and human islets transfected with TXNIP **(f)**. **(g,h)** Insulin content **(g)** and insulin secretion **(h)** assessed by ELISA in INS-TXNIP and INS-LacZ control cells. **(i)** Islet insulin content measured by ELISA in primary islets of TXNIP-deficient HcB-19 and control C3H mice. **(j)** Insulin content, measured by ELISA and normalized for DNA content, in control C3H and TXNIP-deficient HcB-19 mouse islets that were transfected with scrambled control microRNA or precursor miR-204 and analyzed 2 d later. All data are shown as the mean \pm s.e.m. of three independent experiments. * $P < 0.05$, ** $P < 0.01$ (Student's *t* test **(a–h)** or analysis of variance **(j)**). NS, not significant.

production. To further obtain direct evidence for the role of miR-204 in this process, we overexpressed miR-204 in islets of *Txnip*-deficient mice, which completely blunted the effect of the lack of *Txnip* and reduced islet insulin content to amounts comparable with those in wild-type control mice (Fig. 4j). This rescue experiment further established the causal relationship between decreased TXNIP and miR-204 expression and increased insulin production and revealed an important functional link suggesting that TXNIP inhibits insulin production through the induction of miR-204 expression.

On the basis of our discovery that TXNIP inhibits STAT3 activation and STAT3 inhibition in turn increases miR-204 expression, we also investigated the possibility that STAT3 inhibition could regulate insulin production. Both insulin and *Mafa* expression were significantly ($P < 0.01$) reduced in response to STAT3 inhibition (Supplementary Fig. 5e,f), providing additional evidence for the importance of this newly identified pathway in conferring the observed effects of TXNIP.

Because miR-204 and *TRPM3* are co-regulated by TXNIP, we addressed the question of whether any of the observed effects might be mediated by TRPM3. We therefore knocked down *Trpm3* using siRNA and assessed whether this could mimic the effects of miR-204 inhibition. However, although we found a robust downregulation of *Trpm3* (Supplementary Fig. 5g), the expression of neither *Mafa* (Supplementary Fig. 5h) nor insulin (Supplementary Fig. 5i) was increased and, in contrast to the results of miR-204 inhibition, were instead decreased. This result indicates that TRPM3 does not confer the observed TXNIP-mediated inhibition of insulin transcription. Moreover, it also suggests that miR-204 is able to not only regulate insulin transcription, as demonstrated by miR-204 overexpression and inhibition, but, in the case of TXNIP overexpression, also outweigh the opposing effects of TRPM3.

Taken together, our findings in INS-1 beta cells, islets of *Txnip*-deficient mice, diabetic mouse models and primary human islets demonstrate that TXNIP inhibits STAT3 and induces beta-cell transcription of a specific microRNA, miR-204, which in turn blocks insulin production by directly targeting and downregulating the crucial transcription factor MAFA. This suggests that the TXNIP-phosphorylated STAT3 (pSTAT3)–miR-204–MAFA–insulin pathway may contribute to impaired insulin production, beta-cell dysfunction and the pathogenesis of diabetes (Supplementary Fig. 6).

Whereas our previous work revealed the important role of TXNIP in diabetic beta-cell death^{2,3,8,11}, our current results demonstrate that TXNIP also controls *in vivo* beta-cell function and insulin production. The higher insulin production associated with TXNIP deficiency might have contributed to the antidiabetic effects observed³ and may provide an added bonus when targeting TXNIP as a therapeutic approach for diabetes. Our current findings are also consistent with a previous report that showed an association of changes in TXNIP expression with altered insulin secretion³⁴.

We previously found that *Txnip*-deficient HcB-19 mice also have significantly ($P < 0.05$) lower blood glucose concentrations and are protected against streptozotocin- and obesity-induced diabetes³. On the basis of the newly identified signaling pathway in which TXNIP induces miR-204 expression and thereby downregulates MAFA and insulin production, one would anticipate that *Mafa* knockout mice would have a phenotype that is opposed to that of *Txnip*-deficient mice. Indeed, *Mafa* knockout mice are characterized by lower insulin transcription and higher blood glucose concentrations, and at ~1 year of age many *Mafa* knockout mice progress spontaneously to overt diabetes with blood glucose concentrations of over 500 mg dl⁻¹ (ref. 35).

These data are not only consistent with our current findings but also underline the importance that this TXNIP–miR-204–MAFA–insulin signaling cascade seems to have in the physiology and pathophysiology of glucose homeostasis in a whole animal.

Because we discovered that TXNIP downregulates STAT3 phosphorylation and activation, which results in increased miR-204 expression and decreased insulin production, *STAT3* deletion would be predicted to impair glucose homeostasis. Indeed, pancreas-specific *Stat3* knockout mice show glucose intolerance and impaired insulin secretion³⁶, providing additional *in vivo* support for the new pathway we identified here.

Although multiple microRNAs have been implicated in beta-cell biology^{15–21} and insulin gene expression^{18,37–39}, miR-204 has not been one of them. Nevertheless, in a study looking at microRNA patterns to distinguish between different pancreatic tumor types, miR-204 was found to be highly expressed in insulinomas and to correlate with immunohistochemical expression of insulin²², which is commonly used as a marker to define the beta-cell origin of these tumors. In this context, it is also important to note that the high systemic concentrations of insulin found in patients with insulinomas are due primarily to neoplastic growth and an abnormal increase in the number of insulin-producing beta cells giving rise to the tumor and not necessarily to increased insulin production per beta cell. The observed correlation is therefore not able to provide any information about the regulation of insulin expression by miR-204 and simply underlines the predominant beta-cell expression pattern of miR-204 and, as stated by the authors of the previous study²², its potential usefulness in distinguishing insulinomas from other pancreatic tumors. As such, their study is in line with our findings.

The discovery that miR-204 is upregulated in diabetes and controls insulin transcription reveals a potential new target for the future development of RNA therapeutics that would address an unmet need for increasing insulin production. Silencing of microRNAs has just begun to be explored for the treatment of cancers and various other diseases, including diabetes⁴⁰. In addition, the observation that TXNIP controls microRNA expression, which can in turn regulate key transcription factors such as MAFA and thereby perhaps modulate cell function and differentiation, fundamentally changes our understanding of the role TXNIP and microRNA biology have in health and disease.

METHODS

Methods and any associated references are available in the [online version of the paper](#).

Note: Any Supplementary Information and Source Data files are available in the online version of the paper.

ACKNOWLEDGMENTS

This work was supported by grants to A.S. from the US National Institutes of Health (R01DK-078752), the American Diabetes Association (7-12-BS-167) and the Juvenile Diabetes Research Foundation and JNJSI (40-2011-1). A-ZIP/F mice were a generous gift of C. Vinson, US National Institutes of Health.

AUTHOR CONTRIBUTIONS

G.X. designed, performed and analyzed the experiments and helped prepare the manuscript. J.C. was responsible for the mouse studies and islet isolations. G.J. performed most of the cloning and helped with some of the experiments. A.S. conceived the project, supervised the work and wrote the manuscript.

COMPETING FINANCIAL INTERESTS

The authors declare no competing financial interests.

Reprints and permissions information is available online at <http://www.nature.com/reprints/index.html>.

1. Poitout, V. & Robertson, R.P. Minireview: secondary beta-cell failure in type 2 diabetes—a convergence of glucotoxicity and lipotoxicity. *Endocrinology* **143**, 339–342 (2002).
2. Chen, J., Saxena, G., Mungrue, I.N., Lusi, A.J. & Shalev, A. Thioredoxin-interacting protein: a critical link between glucose toxicity and beta cell apoptosis. *Diabetes* **57**, 938–944 (2008).
3. Chen, J. *et al.* Thioredoxin-interacting protein deficiency induces Akt/Bcl-xL signaling and pancreatic beta cell mass and protects against diabetes. *FASEB J.* **22**, 3581–3594 (2008).
4. Courboulin, A. *et al.* Role for miR-204 in human pulmonary arterial hypertension. *J. Exp. Med.* **208**, 535–548 (2011).
5. Paulin, R. *et al.* Dehydroepiandrosterone inhibits the Src/STAT3 constitutive activation in pulmonary arterial hypertension. *Am. J. Physiol. Heart Circ. Physiol.* **301**, H1798–H1809 (2011).
6. Nishiyama, A., Masutani, H., Nakamura, H., Nishinaka, Y. & Yodoi, J. Redox regulation by thioredoxin and thioredoxin-binding proteins. *IUBMB Life* **52**, 29–33 (2001).
7. Shalev, A. *et al.* Oligonucleotide microarray analysis of intact human pancreatic islets: identification of glucose-responsive genes and a highly regulated TGF β signaling pathway. *Endocrinology* **143**, 3695–3698 (2002).
8. Minn, A.H., Hafele, C. & Shalev, A. Thioredoxin-interacting protein is stimulated by glucose through a carbohydrate response element and induces beta-cell apoptosis. *Endocrinology* **146**, 2397–2405 (2005).
9. Minn, A.H. *et al.* Gene expression profiling in INS-1 cells overexpressing thioredoxin-interacting protein. *Biochem. Biophys. Res. Commun.* **336**, 770–778 (2005).
10. Saxena, G., Chen, J. & Shalev, A. Intracellular shuttling and mitochondrial function of thioredoxin-interacting protein. *J. Biol. Chem.* **285**, 3997–4005 (2010).
11. Chen, J., Fontes, G., Saxena, G., Poitout, V. & Shalev, A. Lack of TXNIP protects against mitochondria-mediated apoptosis but not against fatty acid-induced ER stress-mediated beta-cell death. *Diabetes* **59**, 440–447 (2010).
12. Sun, Y. *et al.* Development of a micro-array to detect human and mouse microRNAs and characterization of expression in human organs. *Nucleic Acids Res.* **32**, e188 (2004).
13. Landgraf, P. *et al.* A mammalian microRNA expression atlas based on small RNA library sequencing. *Cell* **129**, 1401–1414 (2007).
14. Winter, J., Jung, S., Keller, S., Gregory, R.I. & Diederichs, S. Many roads to maturity: microRNA biogenesis pathways and their regulation. *Nat. Cell Biol.* **11**, 228–234 (2009).
15. Fernandez-Valverde, S.L., Taft, R.J. & Mattick, J.S. MicroRNAs in beta-cell biology, insulin resistance, diabetes and its complications. *Diabetes* **60**, 1825–1831 (2011).
16. Kantharidis, P., Wang, B., Carew, R.M. & Lan, H.Y. Diabetes complications: the microRNA perspective. *Diabetes* **60**, 1832–1837 (2011).
17. Lynn, F.C. *et al.* MicroRNA expression is required for pancreatic islet cell genesis in the mouse. *Diabetes* **56**, 2938–2945 (2007).
18. Melkman-Zehavi, T. *et al.* miRNAs control insulin content in pancreatic beta-cells via downregulation of transcriptional repressors. *EMBO J.* **30**, 835–845 (2011).
19. Poy, M.N. *et al.* A pancreatic islet-specific microRNA regulates insulin secretion. *Nature* **432**, 226–230 (2004).
20. Poy, M.N. *et al.* miR-375 maintains normal pancreatic alpha- and beta-cell mass. *Proc. Natl. Acad. Sci. USA* **106**, 5813–5818 (2009).
21. Tattikota, S.G. & Poy, M.N. Re-dicing the pancreatic beta-cell: do microRNAs define cellular identity? *EMBO J.* **30**, 797–799 (2011).
22. Roldo, C. *et al.* MicroRNA expression abnormalities in pancreatic endocrine and acinar tumors are associated with distinctive pathologic features and clinical behavior. *J. Clin. Oncol.* **24**, 4677–4684 (2006).
23. Krol, J. *et al.* Characterizing light-regulated retinal microRNAs reveals rapid turnover as a common property of neuronal microRNAs. *Cell* **141**, 618–631 (2010).
24. Xu, G., Chen, J., Jing, G. & Shalev, A. Preventing beta-cell loss and diabetes with calcium channel blockers. *Diabetes* **61**, 848–856 (2012).
25. Clee, S.M., Nadler, S.T. & Attie, A.D. Genetic and genomic studies of the BTBR ob/ob mouse model of type 2 diabetes. *Am. J. Ther.* **12**, 491–498 (2005).
26. Moitra, J. *et al.* Life without white fat: a transgenic mouse. *Genes Dev.* **12**, 3168–3181 (1998).
27. Artner, I. *et al.* MafA and MafB regulate genes critical to beta-cells in a unique temporal manner. *Diabetes* **59**, 2530–2539 (2010).
28. Le Lay, J. & Stein, R. Involvement of PDX-1 in activation of human insulin gene transcription. *J. Endocrinol.* **188**, 287–294 (2006).
29. Sharma, A. *et al.* The NeuroD1/BETA2 sequences essential for insulin gene transcription colocalize with those necessary for neurogenesis and p300/CREB binding protein binding. *Mol. Cell Biol.* **19**, 704–713 (1999).
30. Vanhooose, A.M. *et al.* MafA and MafB regulate Pdx1 transcription through the area II control region in pancreatic beta cells. *J. Biol. Chem.* **283**, 22612–22619 (2008).
31. Matsuoka, T.A. *et al.* Regulation of MafA expression in pancreatic beta-cells in db/db mice with diabetes. *Diabetes* **59**, 1709–1720 (2010).
32. Vanderford, N.L., Andrali, S.S. & Ozcan, S. Glucose induces MafA expression in pancreatic beta cell lines via the hexosamine biosynthetic pathway. *J. Biol. Chem.* **282**, 1577–1584 (2007).
33. Lewis, B.P., Burge, C.B. & Bartel, D.P. Conserved seed pairing, often flanked by adenosines, indicates that thousands of human genes are microRNA targets. *Cell* **120**, 15–20 (2005).
34. Rani, S. *et al.* Decreasing Txnip mRNA and protein levels in pancreatic MIN6 cells reduces reactive oxygen species and restores glucose regulated insulin secretion. *Cell Physiol. Biochem.* **25**, 667–674 (2010).
35. Zhang, C. *et al.* MafA is a key regulator of glucose-stimulated insulin secretion. *Mol. Cell Biol.* **25**, 4969–4976 (2005).
36. Kostromina, E. *et al.* Glucose intolerance and impaired insulin secretion in pancreas-specific signal transducer and activator of transcription-3 knockout mice are associated with microvascular alterations in the pancreas. *Endocrinology* **151**, 2050–2059 (2010).
37. Bolmeson, C. *et al.* Differences in islet-enriched miRNAs in healthy and glucose intolerant human subjects. *Biochem. Biophys. Res. Commun.* **404**, 16–22 (2011).
38. El Ouaamari, A. *et al.* miR-375 targets 3'-phosphoinositide-dependent protein kinase-1 and regulates glucose-induced biological responses in pancreatic beta-cells. *Diabetes* **57**, 2708–2717 (2008).
39. Zhao, X., Mohan, R., Ozcan, S. & Tang, X. MicroRNA-30d induces insulin transcription factor MafA and insulin production by targeting mitogen-activated protein 4 kinase 4 (MAP4K4) in pancreatic beta-cells. *J. Biol. Chem.* **287**, 31155–31164 (2012).
40. Krützfeldt, J. *et al.* Silencing of microRNAs *in vivo* with 'antagomirs'. *Nature* **438**, 685–689 (2005).

ONLINE METHODS

Tissue culture. INS-1 beta cells and stably transfected INS-TXNIP human or control INS-LacZ cells were grown as previously described⁸. INS-1 cells were treated with the STAT3 inhibitor STAT3IC (sc-202818, Santa Cruz Biotechnology, Santa Cruz, CA) as indicated. Mouse pancreatic islets were isolated by collagenase digestion as detailed previously². Human islets were obtained from the UAB Islet Resource Facility, islets from the same donor were used as controls, and islets from at least three different donors were used per experiment.

Animal studies. All mouse studies were approved by the University of Alabama at Birmingham Animal Care and Use Committee and conformed to the US National Institutes of Health Guide for the Care and Use of Laboratory Animals. The C3H congenic *Txnip*-deficient HcB-19 (HcB) mice harboring a naturally occurring nonsense mutation in the *Txnip* gene and the control C3H/DiSnA (C3H) strain, as well as beta cell-specific *Txnip* knockout mice (bTKO) and the corresponding controls (*lox/lox*), have been described previously³. Male 1-year-old mice were used for the studies described here.

Plasmid construction, transfection and luciferase assays. The TXNIP expression plasmid has been described previously⁸. The human insulin promoter region was amplified from genomic DNA with the primers listed in **Supplementary Table 2** and was subcloned into the *Mlu*I and *Hind*III restriction sites of the pGL3 enhancer vector (Promega, Madison, WI), producing the *Ins*-luc reporter plasmid. The wild-type rat *Mafa* 3' UTR region containing the miR-204 binding site was amplified from rat genomic DNA using primers designed on the basis of the sequence in the UCSC genome browser (<http://genome.ucsc.edu>) between the stop codon and the poly(A) site of rat *Mafa* (**Supplementary Table 2**). The human *MAFA* 3' UTR was cloned on the basis of the sequence in NCBI (NM_201589). To generate the *MAFA* mutant reporter plasmids, mutations were introduced by PCR and the primers listed in **Supplementary Table 2**. PCR products were subcloned into the *Spe*I and *Pme*I sites of the pMIR-REPORT luciferase vector (Applied Biosystems, Foster City, CA), yielding the rat *Mafa*-WT-3'Luc and *Mafa*-M-3'Luc 3'UTR reporter plasmids, as well as the human plasmids h*MAFA*-WT-3'Luc and h*MAFA*-M-3'Luc. All plasmids were confirmed by sequencing. The presence of the predicted rat and mouse *Mafa* 3' UTR sequences was also confirmed using RNA from rat INS-1 beta cells and mouse islets and the 3' System for Rapid Amplification of cDNA Ends (RACE) (Invitrogen, Grand Island, NY). For transfection experiments, INS-1 cells were plated in six-well plates and grown overnight to ~60% confluence. Human islets (500 per tube) or mouse islets (100 per tube) were gently dispersed by incubation for 5 min in 200 μ l of 0.05% trypsin-EDTA (Invitrogen) at 37 °C, washed and resuspended in culture medium. Cells were transfected with hsa-miR-204 precursor or pre-miR negative control 2 (Applied Biosystem) at a final concentration of 25 nM using the DharmaFECT1 transfection reagent (Dharmacon/Thermo Scientific, Chicago, IL). For luciferase assays, INS-1 cells (or human HEK293 cells) were grown overnight in 12-well plates and cotransfected with *Ins*-Luc, *Mafa*-WT-3'Luc or *Mafa*-M-3'Luc (or h*MAFA*-WT-3'Luc or h*MAFA*-M-3'Luc) and hsa-miR-204 or a negative control using the DharmaFECTDuo transfection reagent (Dharmacon/Thermo Scientific). To control for transfection efficiency, cells were cotransfected with the pRL-TK (Promega) control plasmid expressing

Renilla luciferase, and firefly as well as *Renilla* luciferase activity were determined using the Dual Luciferase Assay Kit (Promega).

Quantitative real-time RT-PCR. qRT-PCR was performed as described previously³ using a LightCycler 480 system (Roche, Indianapolis, IN) and the primers listed in **Supplementary Table 2**. miR-204 expression was quantified using a TaqMan microRNA Assay (Applied Biosystems). Gene and microRNA expression results were corrected for 18S and U6 (or small nucleolar RNA-135 (snoRNA-135) for comparisons involving diabetic mouse models), respectively, which were run as internal standards. Internal standards were stable throughout all experiments, and the experiments were run in duplicates.

Immunoblotting. Protein extracts were prepared and analyzed as described previously². MAFA was detected using rabbit antibody to MAFA (1:500) (sc-66958X, Santa Cruz Biotechnology, Santa Cruz, CA). Total and pSTAT3 were detected using rabbit antibody to STAT3 (1:1,000) (4904, Cell Signaling Technology, Danvers, MA) and rabbit pSTAT3-specific antibody (1:1,000) (9145, Cell Signaling Technology).

Insulin content and secretion. Insulin content and secretion in isolated islets and INS-1 cells were assessed by ELISA and normalized for DNA content as described previously². In brief, INS-1 cells were plated in 24-well plates, and after overnight incubation in 5 mM glucose, the medium was removed and the cells were incubated in Krebs ringer bicarbonate (KRB) buffer (135 mM NaCl, 3.6 mM KCl, 10 mM 4-(2-hydroxyethyl)-1-piperazineethanesulfonic acid (HEPES), pH 7.4, 5 mM NaHCO₃, 0.5 mM NaH₂PO₄, 0.5 mM MgCl₂ and 1.5 mM CaCl₂) with 2.5 mM glucose for 1 h. After stimulation with KRB buffer containing 16.7 mM glucose for 1 h, the medium was harvested for later insulin assay. Cells were lysed with 300 μ l lysis buffer (100 mM Tris-HCl, pH 8.0, 300 mM NaCl, 10 mM NaF, 2 mM Na orthovanadate, 2% NP-40 and two protease cocktail tablets (Roche)), and lysates were stored overnight at -20 °C. After centrifugation at 5,000 r.p.m. for 5 min, the supernatants were harvested for insulin assay with the Ultra Sensitive Rat Insulin ELISA Kit (Crystal Chem Inc., Downers Groves, IL), and transfected mouse islets were analyzed with the Mouse Insulin Assay kit (ALPCO Diagnostics, Salem, NH). Results were normalized for DNA content, as determined by Quant-iTPicoGreensDNA Assay kit (Invitrogen).

ChIP. ChIP assays were performed as described previously⁴¹. Five micrograms of rabbit antibody to MAFA (A300-611A, Bethyl Laboratories, Montgomery, TX) or normal rabbit IgG (sc-2027, Santa Cruz) were used for immunoprecipitation, and purified DNA fragments were quantified by qPCR with the primers listed in **Supplementary Table 2**.

Statistical analyses. Student's *t* test or one-way analysis of variance was used to calculate the significance of a difference between two groups or between more than two groups, respectively.

41. Cha-Molstad, H., Saxena, G., Chen, J. & Shalev, A. Glucose-stimulated expression of *Txnip* is mediated by carbohydrate response element-binding protein, p300, and histone H4 acetylation in pancreatic beta cells. *J. Biol. Chem.* **284**, 16898–16905 (2009).